Schleh Michael W (Orcid ID: 0000-0001-9969-6316)

Metabolic dysfunction in obesity is related to impaired suppression of fatty acid release from adipose tissue by insulin

Michael W. Schleh[1,*], Benjamin J. Ryan[1,*], Cheehoon Ahn[1], Alison C. Ludzki[1], Pallavi Varshney[1], Jenna B. Gillen[1,2], Douglas W. Van Pelt[1], Lisa M. Pitchford[1], Suzette M. Howton[1], Thomas Rode[1], Thomas L. Chenevert[3], Scott L. Hummel[4,5], Charles F. Burant[6], Jeffrey F. Horowitz[1]

[1] Substrate Metabolism Laboratory, School of Kinesiology, University of Michigan, Ann Arbor, Michigan, USA

[2] Faculty of Kinesiology and Physical Education, University of Toronto, Toronto, Ontario, Canada

[3] Department of Radiology, University of Michigan, Ann Arbor, Michigan, USA

[4] Division of Cardiology, Department of Internal Medicine, University of Michigan, Ann Arbor, Michigan, USA

[5] Veterans Affairs Health System, Ann Arbor, Michigan, USA

[6] Division of Metabolism, Endocrinology, and Diabetes, Department of Internal Medicine, University of Michigan, Ann Arbor, Michigan, USA

* Co-first author

Running title: Adipose tissue and insulin sensitivity

Keywords: Adipose tissue, extracellular matrix, insulin sensitivity, obesity, skeletal muscle.

Corresponding author: Jeffrey Horowitz, PhD; School of Kinesiology, University of Michigan, 830 North University, Ann Arbor, MI 48109, USA. Email: jeffhoro@umich.edu

Clinical trial registration: clinicaltrials.gov; NCT02717832, NCT02706093

Funding: National Institutes of Health (R01DK077966, P30DK089503, U24DK097153, T32DK007245, F32DK117522), American Diabetes Association (1-16-ICTS-048), and the Canadian Institutes of Health Research (338735 and 146190).

Disclosure: The authors declared no conflict of interest

Author contributions: MWS, BJR, CA, ACL, JBG, DVP, LMP, and TR contributed to study design and performed data acquisition. SMH coordinated participant recruitment. MWS performed data analysis and interpretation of the data. MWS and JFH drafted the manuscript. All authors read and revised the final version of the article to be published and have provided final approval.

ORCiD identifiers: 0000-0001-9969-6316 (M. W. Schleh); 0000-0001-5848-6988 (B. J. Ryan); 0000-0003-4140-125X (C. Ahn); 0000-0002-6967-034X (A. C. Ludzki); 0000-0001-9594-604X (D. W. Van Pelt); 0000-0002-6402-0823 (L. M. Pitchford); 0000-0002-0924-3135 (S. Hummel); 0000-0003-3851-777X (J. F. Horowitz).

Study Importance

What is already known about this subject?

- Rates of fatty acid release from abdominal subcutaneous adipose tissue (aSAT) can vary considerably among individuals with obesity.
- Excessive rates fatty acid release from aSAT, and resultant uptake into metabolically active tissues such as skeletal muscle and liver, are key factors underlying the development of insulin resistance in obesity.

What are the new findings?

- The suppression of fatty acid rate of appearance in response to insulin (FA Ra suppression) associated with insulin-mediated glucose uptake, and the ectopic accumulation of long-chain acylcarnitine and triacylglycerol in skeletal muscle.
- Factors associated with aSAT morphology – such as smaller adipocyte size and lower ECM fibrosis – may contribute to enhanced FA Ra suppression in response to insulin.

How might your results change the direction of research or the focus of clinical practice?

- Greater FA Ra suppression in response to insulin may be attributed to lower aSAT fibrosis and adipocyte size in adults with obesity, and greater metabolic health outcomes.

Abstract

Objectives: 1) Assess relationships between insulin-mediated glucose uptake with standard clinical outcomes, and deep-phenotyping measures (including FA rate of appearance (FA Ra) into the systemic circulation); and 2) examine the contribution of adipocyte size, fibrosis, and proteomic profile to FA Ra regulation.

Methods: Sixty-six adults with obesity (BMI=34±3 kg/m^2) were assessed for insulin sensitivity (hyperinsulinemic-euglycemic clamp), and stable isotope dilution methods quantified glucose, FA, and glycerol kinetics in vivo. Abdominal subcutaneous adipose tissue (aSAT) and skeletal muscle biopsies were collected, and MRI quantified liver and visceral fat content.

Results: Insulin-mediated FA Ra suppression associated with insulin-mediated glucose uptake ($r=0.51$; $p<0.01$), and negatively correlated with liver ($r=-0.36$; $p<0.01$) and visceral fat ($r=-0.42$; $p<0.01$). aSAT proteomics from sub-cohorts of participants with Low FA Ra suppression (LS; n=8) versus High FA Ra suppression (HS; n=8) demonstrated greater ECM collagen protein in LS versus HS. Skeletal muscle lipidomics (n=18) revealed inverse correlations between FA Ra suppression with acyl-chain length of acylcarnitine ($r=-0.42$; $p=0.02$) and triacylglycerol ($r=-0.51$; $p<0.01$), in addition to insulin-mediated glucose uptake (acylcarnitine: $r=-0.49$; $p<0.01$, triacylglycerol: $r=-0.40$; $p<0.01$).

Conclusion: Insulin's ability to suppress FA release from aSAT in obesity is related to enhanced insulin-mediated glucose uptake, and metabolic health in peripheral tissues.

Introduction

Impaired insulin-mediated glucose uptake (i.e., insulin resistance) underlies many obesity-related diseases (1). Although most adults with obesity are resistant to the glucose lowering effects of insulin, up to 30% of adults with obesity remain relatively insulin sensitive, with minimal metabolic health complications (2). Why some adults with obesity are profoundly resistant to insulin-mediated glucose uptake, while others are relatively insulin sensitive, remains elusive. Findings from our lab (3, 4) and others (5, 6) suggest maintaining low FA mobilization rates into the systemic circulation may 'protect' some adults with obesity from developing insulin resistance. The majority of FA delivered into the systemic circulation are derived from subcutaneous adipose tissue (SAT) depots localized to the upper body, rather than gluteal or visceral depots (7). The rate of FA mobilization from abdominal SAT (aSAT) into the systemic circulation is primarily determined by triacylglycerol (TAG) hydrolysis (lipolysis), and the rate at which FAs liberated by lipolysis are re-incorporated into TAG within adipocytes (re-esterification). While these processes are largely regulated by lipase and acyltransferase enzyme activity, other factors such as aSAT morphology (size, vascularization, fibrosis), and local and systemic inflammation may also impact FA release (8, 9).

The metabolic consequences of excessively high FA availability contributes to high FA uptake rates and resultant 'ectopic' lipid accumulation in other tissues such as skeletal muscle and liver (10). High rates of FA uptake into the liver can impair hepatic insulin sensitivity and lead to the development of chronic liver disorders (nonalcoholic fatty liver disease and steatohepatitis). Because skeletal muscle is the primary site of insulin-mediated glucose uptake (11), preservation of skeletal muscle insulin action is central for

maintaining whole-body glucose control. Excessive FA uptake into skeletal muscle can lead to a local accumulation of lipid intermediates, including diacylglycerol (DAG) (12), ceramide (13), and long-chain acyl-CoA (14, 15), which have been causally linked with insulin resistance. Additionally, the conformation of lipid species, such as acyl-chain length (16) and saturation (17), have also been implicated in skeletal muscle insulin signaling. Given the important repercussions of high FA uptake and lipid accumulation in ectopic tissues, an enhanced ability to sequester FA in aSAT appears metabolically favorable. However, relationship between aSAT FA mobilization and lipid accumulation in these tissues remains unresolved.

The primary aims of this study were to: 1) assess relationships between insulin-mediated glucose uptake with standard clinical outcomes, as well as deep-phenotyping measures, including FA rate of appearance (FA Ra) into the systemic circulation; and 2) examine the potential contribution of adipocyte size, ECM collagen accumulation, and aSAT proteomic profile to FA Ra in adults with obesity and wide-ranging insulin sensitivity. We also examined relationships between FA Ra with lipid accumulation in skeletal muscle, liver, and intra-abdominal tissues adipose tissue.

Methods

Study population

Sixty-six men (n=20) and women (n=46) with obesity (BMI=30-40 kg/m^2) completed the study (Table 1). All participants were weight stable (±2 kg) and sedentary (no planned moderate-to-vigorous exercise for previous 6-months). After completion of the testing reported here, a subset of participants (n=36) subsequently participated in an

exercise training intervention addressing hypotheses unrelated to the present work (18, 19). Participants were not taking medications known to affect glucose or lipid metabolism and did not have a history of heart disease or active smoking. All women were pre-menopausal, eumenorrheic, and not pregnant or lactating. All participants provided written informed consent before participation. The study protocol was approved by the University of Michigan Institutional Review Board, carried out in accordance with the principles of the Declaration of Helsinki, and registered at clinicaltrials.gov (NCT02717832, NCT02706093).

Experimental protocol

Participants consumed a standardized dinner and snack the day before the study trial and arrived to the Michigan Clinical Research Unit (MCRU) at 0700h the following morning (Figure S1 presents study schematic and details). After 30min rest, resting metabolic rate (RMR) and substrate (fat and carbohydrate) oxidation was measured via indirect calorimetry (Vmax; CareFusion, San Diego, CA). RMR (kcal/day) was calculated from the Weir equation (20), and substrate oxidation (g/min) was calculated according to Frayn (21). At ~0800h, intravenous catheters were inserted into the hand/forearm vein for continuous blood sampling, and continuous isotope, insulin, and glucose infusion. At ~0900h, baseline blood samples were collected for background isotope enrichment, followed by primed continuous infusions of [6,6 $^{2}H_{2}$]glucose (35 μmol/kg priming dose, and 0.41 μmol/kg/min continuous infusion), and [$^{2}H_{5}$]glycerol (1.5 μmol/kg priming dose, and 0.1 μmol/kg/min continuous infusion). At ~0915h, skeletal muscle biopsies were collected from the vastus lateralis, and aSAT biopsies were collected by aspiration lateral to the umbilicus. At ~1000h, a continuous [1-^{13}C]palmitate infusion (0.04 μmol/kg/min) began to determine FA kinetics. Three arterialized samples (heated hand technique) were

collected at 1050h, 1055h, and 1100h to determine fasting substrate kinetics. At ~1100h, a 2h hyperinsulinemic-euglycemic clamp procedure began to determine insulin-mediated glucose uptake (40 mU/m^2/min). Continuous blood glucose samples were obtained every 5min (StatStrip, Nova Biomedical, Waltham, MA), and dextrose (20% dextrose, enriched with [6,6^{2}H$_2$]glucose) infusion rates were modified to maintain baseline glucose concentration at ~5 mmol/l. Five blood samples were collected during the last 20min of the clamp to determine insulin-mediated substrate kinetics.

Body composition, liver fat, and visceral fat area.

Body composition was assessed by DEXA (Lunar DPX, GE Healthcare, Madison, WI) at MCRU. Visceral fat area and liver fat percentage were measured by MRI (Ingenia 3T; Philips, Amsterdam) at the University of Michigan, Department of Radiology. MRI images were captured by chemical shift–encoded MRI proton density fat fraction (22), and image acquisition as described previously (18). Visceral fat area was measured from 3, 5-mm axial slices between L2-L3 interspace, and liver fat percentage was measured from 3, 5-mm liver axial slices. Both liver and visceral fat area were quantified by a trained investigator blinded to participant identification.

Participant stratification into High versus Low FA Ra suppression sub-cohorts

For paired analyses, a sub-cohort of participants were stratified into High FA Ra suppression (HS) or Low FA Ra suppression (LS) sub-cohorts based on percent change in FA Ra from baseline to hyperinsulinemia during the clamp (HS=85±2%, LS=63±6% FA Ra suppression by insulin; n=8 per sub-cohort). Importantly, participants selected for sub-cohort stratification were strictly matched for sex and fat mass to avoid confounding effects of these parameters on metabolic health (Table 1).

Plasma glucose, glycerol, and FA kinetics.

Tracer-to-tracee ratios (TTR) quantified glucose, palmitate, and glycerol kinetics by gas chromatography mass spectrometry (GC-MS) and described in Methods S1. Kinetics were calculated respective to TTR from each substrate by the Steele equation for steady state conditions (23). FA Ra was quantified by dividing palmitate Ra by the ratio of total palmitate (C16:0) to FAs within a standard, as described previously (3, 4).

Adipocyte size and fibrosis.

Adipocytes were stained by Harris's hematoxylin (Sigma-Aldrich, St. Louis, MO) and eosin (Sigma-Aldrich) as described previously by our lab (19). Adipocyte size was quantified using Image J (NIH, Bethesda, MD) as described previously (24). Large and small adipocyte distributions were determined by the lowest quartile (Q1; 1000-3196μm^2) and highest (Q4; >6784μm^2) from the entire cohort. For fibrosis measurements, picro sirius red stained samples were normalized to tissue surface area from 10 random fields at 10x magnification as described previously (25).

Plasma metabolite, cytokine, and hormone concentration

Plasma glucose, non-esterified fatty acid (NEFA), TAG, high-density lipoprotein (HDL), and cholesterol were measured using commercially available colorimetric assays. Plasma IL-6, C-reactive protein (CRP), leptin, total adiponectin, and high molecular-weight (HMW) adiponectin were measured by ELISA. Insulin was measured by radioimmunoassay. Table S1 includes vendor details.

aSAT proteomics

Liquid chromatography-tandem mass spectrometry (LC-MS/MS) proteomics analysis and quantification were completed by the Proteomics Resource Facility at the University of Michigan, Department of Pathology (described in Methods S2).

Skeletal muscle lipidomics

Untargeted lipidomic analysis was completed by the Michigan Regional Comprehensive Metabolomics Resource Core and described in Methods S3.

Statistical Analysis

All data were tested for normality (Shapiro-Wilk) and log transformed for non-normal distributions. For multivariate analyses, net elastic regression (LASSO) was used to subset clinical and deep phenotyping factors associated with insulin-mediated glucose uptake using *glmnet* package in R. Univariate analysis independently correlating all measured variables and insulin-mediated glucose uptake was analyzed by Pearson's correlation; adjusted for age and sex using *psych* package. Our univariate correlations were also corrected for multiple comparisons using the Benjamini-Hochberg method (26), and represented as p.adjust in the results text. Student's t-tests compared metabolic outcomes in HS versus LS. For proteomic analysis, differential abundance was analyzed using *LIMMA*. Proteins with $p<0.05$ and abundance ratio>1.5 between groups were considered significantly different in abundance. For lipidomic analysis, lipids either negatively or positively associated with both insulin-mediated glucose uptake and FA Ra suppression were displayed based on significance adjusted for multiple comparisons (26). β-coefficients for standardized abundance (z-score) of individual lipid species with respect to acyl-chain length and unsaturation were correlated with standardized rates of insulin-mediated glucose uptake and FA Ra suppression (β_z). Correlations between β_z versus acyl-chain length, and β_z versus unsaturation were correlated by Pearson's. Statistical analysis was completed using R 4.1.0.

RESULTS

Study participants

Participant characteristics are presented in Table 1. All participants had obesity, yet were normoglycemic (HbA1c<5.7%). Despite being homogeneous for body composition and most clinical measures, insulin-mediated glucose uptake and lipid kinetics varied widely among the entire study population (Figure 1A-G).

Clinical and deep phenotyping factors associated with insulin-mediated glucose uptake.

Multiple linear regression for clinical outcomes indicated HMW adiponectin, HDL, and total adiponectin directly correlated with insulin-mediated glucose uptake (non-zero coefficients from LASSO regression), while BMI, plasma TAG, visceral fat area, and liver fat percentage inversely correlated with insulin-mediated glucose uptake (Figure 2A; Table S2 contains complete explanatory variable list). For deep phenotyping outcomes, insulin-mediated FA Ra suppression (expressed as percent change from basal FA Ra), basal hepatic glucose production (glucose Ra), fat oxidation, insulin-mediated suppression of hepatic glucose production, and glycerol Ra during the clamp directly correlated with insulin-mediated glucose uptake (Figure 2B). In contrast, FA Ra during the clamp inversely correlated with insulin-mediated glucose uptake (Figure 2B). The subset factors from the LASSO regression were then analyzed by multiple linear regression with the clinical factors model (MODEL 1) and a deep phenotyping factors model (MODEL 2). Both models significantly associated with insulin-mediated glucose uptake (MODEL 1: adjusted R^2=0.21; p<0.01; MODEL 2: adjusted R^2=0.55; p<0.01; Table S3).

Univariate analysis indicated insulin-mediated FA Ra suppression had the strongest positive relationship with insulin-mediated glucose uptake (Figure 2C,D). Importantly, it did not appear that the FA Ra suppression was an artifact of variability in baseline or fasting FA Ra, because the percent change in FA Ra in response to the insulin clamp was not associated with basal FA Ra (r=0.13; p=0.28). In line with the relationship between FA Ra suppression and insulin-mediated glucose uptake, FA Ra during the clamp ("clamp FA Ra") was negatively correlated with insulin-mediated glucose uptake when clamp FA Ra was normalized to fat mass (Figure 2C,E), and fat free mass (Figure 2F).

Adipocyte cell size

Mean adipocyte area inversely associated with both insulin-mediated glucose uptake (r=-0.29, p=0.04; Figure 3A), and FA Ra suppression (r=-0.27, p=0.05; Figure 3B). However, after adjusting for multiple comparisons, statistical significance for these outputs were note maintained (p.adjust = 0.22 and 0.11, respectively). Using quartile stratifications to define small adipocytes (1000-3196μm^2) and large adipocytes (>6784μm^2), we found the proportion of small adipocytes did not associate with insulin-mediated glucose uptake (p=0.18, p.adjust=0.18; Figure 3E) or FA Ra suppression (p= 0.13, p.adjust=0.36; Figure 3F). However, while the correlation between the proportion of large adipocytes and insulin-mediated glucose uptake did not reach statistical significance (Figure 3G), the proportion of large adipocytes inversely correlated with FA Ra suppression (r=-0.28, p=0.04; Figure 3H). This relationship did not quite reach statistical significance after adjusting for multiple comparisons (p.adjust=0.098).

Sub-cohort stratification based on FA Ra suppression

Similar to the wide-ranging insulin-mediated glucose uptake rates among participants, insulin-mediated FA Ra suppression also varied widely (Figure 4A). FA Ra suppression in our HS participants was ~45% greater than LS (HS=82.5-88.0% suppression; LS=50.7-68.5% suppression; Figure 4A). There were no differences in basal FA Ra between sub-cohorts, so the difference in FA Ra suppression was consequential to differences in insulin-mediated FA Ra (Figure 4B). As anticipated, insulin-mediated glucose uptake was significantly greater in HS versus LS, whether normalized to plasma insulin concentration (Figure 4C) or not (Figure 4D). Glucose Ra suppression during the insulin clamp (hepatic insulin sensitivity index) was also greater in HS (Figure 4E,F). Although there were no significant differences in liver fat or visceral fat between sub-cohorts (Figure 4G,H), when we examined this relationship across the entire study cohort, we found significant inverse correlations between FA Ra suppression with both liver fat and visceral ($p<0.01$; Figure 4I,J).

aSAT proteomics

Untargeted proteomics analysis identified 2,519 aSAT proteins (Figure 5A). Of the 2,519 proteins identified, 148 proteins were differentially expressed in HS versus LS (115 proteins were greater in LS, while 33 were greater in HS; Figure 5B,C; Table S4).

ECM-receptor interaction was the highest significant KEGG pathway enriched in LS (Figure 5D). Of proteins within ECM-receptor expression pathway; COL1A1, COL3A1, COL23A1, SEPT5, ITGA2B, and ITGB3 were more abundant in LS versus HS (Figure 5E). In line with this finding, there was an inverse correlation between ECM fibrosis and insulin-mediated glucose uptake across the entire study cohort ($r=-0.37$, $p<0.01$; Figure S2 B). Although we found no significant differences between sub-cohorts for independent

collagen VI isoforms (COL6A1-3), the sum of all COLVI isoforms (∑COL6A1-3) was greater in LS versus HS ($p=0.02$; Figure 5F). Additionally, transforming growth factor β1 (TGFβ1) - a key mediator of fibrosis activated by inflammatory stimuli (27) - was significantly greater in LS ($p=1.18e^{-6}$; Figure 5G).

Skeletal muscle lipidomics

High rates of FA flux from aSAT into the systemic circulation contributes to greater FA uptake into skeletal muscle, accumulating bioactive lipids linked with skeletal muscle insulin resistance. Skeletal muscle lipidomics identified 734 lipid species across all participants, while 21 lipid species significantly correlated with both insulin-mediated glucose uptake and FA Ra suppression (Figure 6A,B; Table S5). Lipids positively correlated with both insulin-mediated glucose uptake and FA Ra suppression consisted primarily of phosphatidylcholine (PC) and phosphatidylethanolamine (PE) species, while lipids inversely correlated with both insulin-mediated glucose uptake and FA Ra suppression included TAG, PC, plasmenyl-PE, and acylcarnitine (Figure 6C). When observing the relationship between insulin-mediated glucose uptake and intra-class lipid abundance, plasmenyl-phosphatidylethanolamine abundance was inversely related with both insulin sensitivity and FA Ra suppression (Figure S3).

In attempt to assess whether relationships existed between the conformation (i.e., acyl-chain length and saturation-state) of key muscle lipids and insulin-mediated glucose uptake or FA Ra suppression, we plotted the β-coefficient values for z-score transformed glucose uptake$_z$ and FA Ra suppression$_z$ versus the standardized abundance of muscle fatty acids (Figure 7A,B), acylcarnitines (Figure 7C,D), DAG (Figure 7E,F), and TAG (Figure 7G,H) for their respective acyl-chain length. Inverse correlations were found for insulin-mediated glucose uptake$_z$ and acyl-chain length of skeletal muscle fatty acids

(p=0.04, p.adjust=0.045; Figure 7A), acylcarnitine (p<0.01, p.adjust<0.01; Figure 7C), and TAG (r=-0.40; p<0.01, p.adjust<0.01; Figure 7G). Inverse correlations between acylcarnitine chain-length and FA Ra suppression$_z$ were also found (r=-0.42; p=0.02, p.adjust=0.03; Figure 7D), while TAG chain length also inversely correlated with FA Ra suppression$_z$ (r=-0.51; p<0.01, p.adjust<0.01; Figure 7H). The same analyses were performed to examine relationships between lipid class saturation with insulin-mediated glucose uptake$_z$ and FA Ra suppression$_z$, and no significant relationships were present (Figure S4).

DISCUSSION

In agreement with work from our lab (3, 4) and others (5, 6), whole body insulin-mediated glucose uptake varied considerably among a relatively homogeneous population of adults with obesity, and the rate of insulin-mediated suppression of FA release from aSAT may help explain this relationship. Because the majority of insulin-mediated glucose uptake occurs in skeletal muscle (11), our findings suggest that the ability for insulin to suppress FA release from aSAT may be an important mediator preserving skeletal muscle insulin sensitivity. Although our correlational analyses do not confirm causality, our findings are consistent with others (5, 6) demonstrating pharmacological reduction in systemic FA mobilization improved insulin-mediated glucose uptake (16). From a clinical perspective, we interpret our findings to suggest enhanced insulin-mediated suppression of FA release may markedly lower FA release from aSAT after meals/snacks when insulin concentrations are high – thereby maintaining systemic FA availability at relatively low levels throughout the day. In turn, limiting

systemic FA availability for ectopic lipid accumulation in insulin responsive tissues, such as skeletal muscle and liver. Our current findings also expand on previous work suggesting aSAT morphology – such as smaller adipocyte size and lower ECM fibrosis – may contribute to enhanced insulin-mediated FA Ra suppression. Additionally, our novel findings suggest that greater insulin-mediated FA Ra suppression – thereby mitigating excessive systemic FA availability – may be contributing to a skeletal muscle lipid phenotype associated with enhanced insulin sensitivity. Overall, our findings suggest an important tissue-specific relationship between adipose tissue with skeletal muscle and liver - by which FA release from aSAT may have important implications on skeletal muscle and liver metabolism.

Excessive FA release from aSAT into the systemic circulation underlies many obesity-related cardiometabolic complications, including insulin resistance (1). Because the majority of FA released into the circulation are derived from aSAT as opposed to visceral depots (7), the regulation of FA metabolism in aSAT is a major contributing factor for obesity-related complications. Our observation that of all parameters measured, insulin-mediated FA Ra suppression had the highest positive correlation with insulin-mediated glucose uptake supports important integrated effects of insulin on both aSAT and skeletal muscle, which is the primary site of insulin-mediated glucose uptake. Therefore, adults with obesity presenting greater sensitivity to suppress insulin-mediated FA release from aSAT may be ‘protected’ from skeletal muscle insulin resistance.

Insulin suppresses FA release from adipose tissue by both inhibiting lipolysis, and stimulating FA re-esterification (28), thereby preventing FA liberated by lipolysis from leaving the adipocyte. Glycerol Ra data from this study (gold-standard measurement for

whole-body lipolysis), suggests that differences in FA Ra suppression among participants were not due to differences in sensitivity to the anti-lipolytic effects of insulin, although we recognize that the relatively high insulin infusion rate may have near-maximally suppressed glycerol Ra in some individuals. Importantly, differences FA re-esterification may help explain the variability in FA Ra suppression, which has been previously reported (29). Intracellular FA re-esterification is largely regulated by the acyltransferase proteins, glycerol 3-phosphate acyltransferase (GPAT) and diacylglycerol acyltransferase (DGAT), and enhanced sensitivity of these proteins in response to insulin may contribute to greater FA Ra suppression. Interestingly, while DGAT activity may be insulin-responsive (30), the effect of insulin on GPAT activity is less clear (31). In addition to the regulation of re-esterification, factors such as aSAT blood flow, and morphological features such as adipocyte size and fibrosis may also contribute to insulin-mediated FA Ra suppression variability (9, 32).

Much of the excess body fat mass in obesity is stored within hypertrophied adipocytes, and the abundance of large adipocytes is an important predictor of insulin resistance and type 2 diabetes (32). FA release from isolated adipocytes in vitro is greater in large adipocytes (33), which aligns with our findings that adipocyte area may inversely associated with insulin-mediated FA Ra suppression. Hypertrophic adipocytes often present elevated pro-inflammatory macrophage accumulation and cytokine release (34), which in turn may attenuate adipose tissue insulin signaling (35), and contribute to lower insulin-mediated FA Ra suppression. Additionally, lower capillary density in hypertrophied adipocytes - and a resultant compromise in microcirculation - may lower insulin delivery, and blunt insulin-mediated FA Ra suppression in vivo.

Highly fibrotic aSAT ECM can also pose physical restrictions for adipocyte expansion during weight gain, and the resulting mechanical stress within the adipocyte has been proposed to increase pro-inflammatory cytokine production (36). Conversely, the reduction of adipose tissue ECM fibrosis in collagen $VI^{-/-}$ mice has been found to markedly reduced inflammatory insult in adipose tissue and vastly improved overall metabolic health (37). Preclinical models have also demonstrated adipose tissue fibrosis attenuates insulin signaling in adipose tissue (37, 38). In humans, the influence for ECM fibrosis to modify insulin signaling or insulin delivery to the adipocyte has been speculated to modify FA mobilization but has not been confirmed to our knowledge. In the current study, our observation that participants in the LS sub-cohort had greater collagen accumulation, supports the prospect that fibrotic aSAT ECM may negatively influence insulin-mediated lipid metabolism.

Interestingly, adipose tissue fibrosis appears to be both a cause and consequence of increased inflammatory stress within the tissue (9, 39). TGFβ1 is implicated in fibrosis development and derived as a result of pro-inflammatory stimuli (39, 40). Activation of TGFβ1 is responsible for progenitor cell differentiation into myofibroblasts and may contribute to increased progenitor cell differentiation away from adipogenesis toward myofibroblast differentiation in ECM (27, 40). Our finding that greater collagen abundance in the LS sub-cohort was accompanied by elevated TGFβ1 aligns with the important role of TGFβ1 in fibrogenesis. Some of the increased inflammatory stimuli that may activate TGFβ1 in adipose tissue can stem from hypoxia induced by low tissue perfusion of hypertrophied adipocytes. Additionally, local hypoxia may increase fibrosis independently of TGFβ1 through HIF1α-mediated activation of platelet-derived growth factor receptor β

progenitor cells towards a myofibroblast lineage (41, 42). Together, hypoxia and inflammatory stimuli may be important factors promoting aSAT ECM fibrosis, and contribute to impaired insulin-mediated FA Ra suppression in aSAT.

Perhaps the most important clinical implication of retaining high insulin-mediated FA Ra suppression is the potential to limit ectopic lipid accumulation. Chronically elevated FA delivery and uptake into liver can result in hepatic steatosis and related disorders, which can greatly impair hepatic glucose metabolism and insulin sensitivity (43). Importantly, our findings that hepatic insulin sensitivity was significantly greater in HS, and that liver fat was inversely correlated with FA Ra suppression across all participants, supports the favorable impact of enhanced insulin-mediated FA Ra suppression on liver metabolism (43). Additionally, although visceral fat accumulation is commonly linked to cardiometabolic complications, much of the fat stored in visceral fat is derived from FA released from aSAT (7). Our findings indicate that visceral fat area inversely correlated with insulin-mediated FA Ra suppression suggests the possibility that this affect may diminish visceral fat, thereby reducing health risks associated with excess visceral fat accumulation.

The link between excessive skeletal muscle FA uptake and insulin resistance has been largely attributed to excess lipid intermediate and metabolite accumulation, such as DAG (12), ceramide (13), and long-chain acyl CoA (14, 15). Although we did not find skeletal muscle DAG or ceramide to be associated with insulin-mediated glucose uptake, our findings that acyl-chain length of fatty acids, acylcarnitines, and TAG in skeletal muscle inversely related with insulin-mediated glucose uptake provides indirect evidence to suggest aberrant lipid metabolism may contribute to impaired skeletal muscle insulin

action. These findings are in general agreement with a previous study demonstrating that lowering 24h FA availability with acipimox (potent lipolytic inhibitor) decreased long-chain fatty acyl-CoA accumulation in skeletal muscle with an accompanying improvement in insulin sensitivity (16). Long-chain lipid accumulation in skeletal muscle can be a consequence of 'incomplete' FA oxidation due to high FA uptake rates and β-oxidation relative to flux through TCA cycle (15), which is very low when sedentary. Although TAG is a neutral lipid, we found long-chain TAG accumulation inversely related with whole-body insulin sensitivity, but the implications of this finding are not clear.

An important limitation of this clinical study is its high reliance on correlational analyses, which hinders our ability to assign causation to integrative interpretations. For example, we suggest impaired insulin-mediated FA Ra suppression from aSAT may precede insulin resistance for glucose metabolism in muscle and liver, but we acknowledge this interpretation is based on correlations. Additionally, although we address the potential role of hypoxia and inflammation on fibrogenesis in aSAT, this supposition was based on prior evidence (41, 42, 44), and direct data to support this notion is not provided. We also acknowledge several other systemic mechanisms may be contributing to low insulin-mediated FA Ra suppression - including sympathetic tone, cellular heterogeneity, and senescence - may be implicated in aSAT dysfunction. Lastly, although the participants in our LS and HS sub-cohorts were sex-matched, we recognize sex differences are important contributing factors to differences observed throughout the entire study cohort.

In summary, our findings indicate greater insulin-mediated suppression of FA release from aSAT may preserve insulin-mediated glucose uptake, hepatic insulin

sensitivity, and lower liver and visceral fat (Figure S5). Together, these findings support the prospect that sustaining the ability for insulin to potently suppress FA release from aSAT may be critical for maintaining metabolic health in adults with obesity. Adipocyte size, aSAT inflammation, and fibrosis may be important mediators of aSAT insulin response. These proposed effects in aSAT may contribute to lower insulin-mediated glucose uptake, perhaps in part through the accumulation of long-chain fatty acid, acylcarnitine, and TAG. Overall, our findings point to an important tissue-specific crosstalk, by which retaining insulin response to suppress FA release from aSAT has impactful metabolic implications in other tissues.

Acknowledgements

We thank the study participants for their efforts; Dr. Benjamin Carr, Dr. Jacob Haus, Jeffrey Wysocki, RN; the staff at MCRU; and all the members of the Substrate Metabolism Lab for study assistance. We would like to thank the Proteomics Resource Facility at the University of Michigan, Department of Pathology, for conducting mass spectrometry experiments; and Michigan Regional Comprehensive Metabolomics Resource Core for conducting lipidomics experiments. Portions of this research are available online as a dissertation (https://dx.doi.org/10.7302/5906).

Data Availability

The source data and R code used for clinical assessment analysis, adipose tissue proteomics, and lipidomics are available upon request with the corresponding authors.

References

1. Reaven GM. Banting lecture 1988. Role of insulin resistance in human disease. *Diabetes* 1988;**37:** 1595-1607.

2. Smith GI, Mittendorfer B, Klein S. Metabolically healthy obesity: facts and fantasies. *J Clin Invest* 2019;**129:** 3978-3989.

3. Van Pelt DW, Guth LM, Wang AY, Horowitz JF. Factors regulating subcutaneous adipose tissue storage, fibrosis, and inflammation may underlie low fatty acid mobilization in insulin-sensitive obese adults. *Am J Physiol Endocrinol Metab* 2017;**313:** E429-E439.

4. Van Pelt DW, Newsom SA, Schenk S, Horowitz JF. Relatively low endogenous fatty acid mobilization and uptake helps preserve insulin sensitivity in obese women. *Int J Obes (Lond)* 2015;**39:** 149-155.

5. Magkos F, Fabbrini E, Conte C, Patterson BW, Klein S. Relationship between Adipose Tissue Lipolytic Activity and Skeletal Muscle Insulin Resistance in Nondiabetic Women. *J Clin Endocrinol Metab* 2012;**97:** E1219-E1223.

6. Koh H-CE, van Vliet S, Pietka TA, Meyer GA, Razani B, Laforest R*, et al.* Subcutaneous adipose tissue metabolic function and insulin sensitivity in people with obesity. *Diabetes* 2021**:** db210160.

7. Nielsen S, Guo Z, Johnson CM, Hensrud DD, Jensen MD. Splanchnic lipolysis in human obesity. *J Clin Invest* 2004;**113:** 1582-1588.

8. Guilherme A, Virbasius JV, Puri V, Czech MP. Adipocyte dysfunctions linking obesity to insulin resistance and type 2 diabetes. *Nat Rev Mol Cell Biol* 2008;**9:** 367-377.

9. Crewe C, An YA, Scherer PE. The ominous triad of adipose tissue dysfunction: inflammation, fibrosis, and impaired angiogenesis. *J Clin Invest* 2017;**127:** 74-82.

10. Unger RH. Lipotoxicity in the pathogenesis of obesity-dependent NIDDM. Genetic and clinical implications. *Diabetes* 1995;**44:** 863-870.

11. DeFronzo RA, Jacot E, Jequier E, Maeder E, Wahren J, Felber JP. The Effect of Insulin on the Disposal of Intravenous Glucose: Results from Indirect Calorimetry and Hepatic and Femoral Venous Catheterization. *Diabetes* 1981;**30:** 1000-1007.

12. Itani SI, Ruderman NB, Schmieder F, Boden G. Lipid-Induced Insulin Resistance in Human Muscle Is Associated With Changes in Diacylglycerol, Protein Kinase C, and IκB-α. *Diabetes* 2002;**51:** 2005-2011.

13. Adams JM, Pratipanawatr T, Berria R, Wang E, DeFronzo RA, Sullards MC*, et al.* Ceramide Content Is Increased in Skeletal Muscle From Obese Insulin-Resistant Humans. *Diabetes* 2004;**53:** 25-31.

14. Ellis BA, Poynten A, Lowy AJ, Furler SM, Chisholm DJ, Kraegen EW*, et al.* Long-chain acyl-CoA esters as indicators of lipid metabolism and insulin sensitivity in rat and human muscle. *Am J Physiol Endocrinol Metab* 2000;**279:** E554-560.

15. Koves TR, Ussher JR, Noland RC, Slentz D, Mosedale M, Ilkayeva O*, et al.* Mitochondrial Overload and Incomplete Fatty Acid Oxidation Contribute to Skeletal Muscle Insulin Resistance. *Cell Metab* 2008;**7:** 45-56.

16. Bajaj M, Suraamornkul S, Romanelli A, Cline GW, Mandarino LJ, Shulman GI*, et al.* Effect of a Sustained Reduction in Plasma Free Fatty Acid Concentration on Intramuscular Long-Chain Fatty Acyl-CoAs and Insulin Action in Type 2 Diabetic Patients. *Diabetes* 2005;**54:** 3148-3153.

17. van Hees AM, Jans A, Hul GB, Roche HM, Saris WH, Blaak EE. Skeletal muscle fatty acid handling in insulin resistant men. *Obesity (Silver Spring, Md)* 2011;**19:** 1350-1359.

18. Ryan BJ, Schleh MW, Ahn C, Ludzki AC, Gillen JB, Varshney P*, et al.* Moderate-intensity exercise and high-intensity interval training affect insulin sensitivity similarly in obese adults. *J Clin Endocrinol Metab* 2020.

19. Ahn C, Ryan BJ, Schleh MW, Varshney P, Ludzki AC, Gillen JB*, et al.* Exercise training remodels subcutaneous adipose tissue in adults with obesity even without weight loss. *J Physiol* 2022;**600:** 2127-2146.

20. Weir JBDB. New methods for calculating metabolic rate with special reference to protein metabolism. *J Physiol* 1949;**109:** 1-9.

21. Frayn KN. Calculation of substrate oxidation rates in vivo from gaseous exchange. *J Appl Physiol Respir Environ Exerc Physiol* 1983;**55:** 628-634.

22. Reeder SB, Cruite I, Hamilton G, Sirlin CB. Quantitative Assessment of Liver Fat with Magnetic Resonance Imaging and Spectroscopy. *J Magn Reson Imaging* 2011;**34:** 729-749.

23. Steele R. Influences of glucose loading and of injected insulin on hepatic glucose output. *Ann N Y Acad Sci* 1959;**82:** 420-430.

24. Parlee SD, Lentz SI, Mori H, MacDougald OA. Quantifying Size and Number of Adipocytes in Adipose Tissue. In: Macdougald OA (ed). *Methods Enzymol*. Academic Press, 2014, pp 93-122.

25. Divoux A, Tordjman J, Lacasa D, Veyrie N, Hugol D, Aissat A*, et al.* Fibrosis in Human Adipose Tissue: Composition, Distribution, and Link With Lipid Metabolism and Fat Mass Loss. *Diabetes* 2010;**59:** 2817.

26. Benjamini Y, Hochberg Y. Controlling the false discovery rate: A practical and powerful approach to multiple testing. *J R Stat Soc* 1995;**57:** 289-300.

27. Keophiphath M, Achard V, Henegar C, Rouault C, Clément K, Lacasa DI. Macrophage-Secreted Factors Promote a Profibrotic Phenotype in Human Preadipocytes. *Mol Endocrinol* 2009;**23:** 11-24.

28. Campbell PJ, Carlson MG, Hill JO, Nurjhan N. Regulation of free fatty acid metabolism by insulin in humans: role of lipolysis and reesterification. *Am J Physiol* 1992;**263:** E1063-1069.

29. Yeckel CW, Dziura J, DiPietro L. Abdominal obesity in older women: potential role for disrupted fatty acid reesterification in insulin resistance. *J Clin Endocrinol Metab* 2008;**93:** 1285-1291.

30. Ali AH, Mundi M, Koutsari C, Bernlohr DA, Jensen MD. Adipose Tissue Free Fatty Acid Storage In Vivo: Effects of Insulin Versus Niacin as a Control for Suppression of Lipolysis. *Diabetes* 2015;**64:** 2828-2835.

31. Chuang S-J, Johanns M, Pyr dit Ruys S, Steinberg GR, Kemp BE, Viollet B*, et al.* AMPK activation by SC4 inhibits noradrenaline-induced lipolysis and insulin-stimulated lipogenesis in white adipose tissue. *Biochem J* 2021;**478:** 3869-3889.

32. Weyer C, Foley JE, Bogardus C, Tataranni PA, Pratley RE. Enlarged subcutaneous abdominal adipocyte size, but not obesity itself, predicts type II diabetes independent of insulin resistance. *Diabetologia* 2000;**43:** 1498-1506.

33. Laurencikiene J, Skurk T, Kulyté A, Hedén P, Åström G, Sjölin E*, et al.* Regulation of Lipolysis in Small and Large Fat Cells of the Same Subject. *J Clin Endocrinol Metab* 2011;**96:** E2045-E2049.

34. Murdolo G, Hammarstedt A, Sandqvist M, Schmelz M, Herder C, Smith U*, et al.* Monocyte chemoattractant protein-1 in subcutaneous abdominal adipose tissue: characterization of interstitial concentration and regulation of gene expression by insulin. *J Clin Endocrinol Metab* 2007;**92:** 2688-2695.

35. Hotamisligil GS, Peraldi P, Budavari A, Ellis R, White MF, Spiegelman BM. IRS-1-mediated inhibition of insulin receptor tyrosine kinase activity in TNF-alpha- and obesity-induced insulin resistance. *Science* 1996;**271:** 665-668.

36. Pellegrinelli V, Heuvingh J, du Roure O, Rouault C, Devulder A, Klein C*, et al.* Human adipocyte function is impacted by mechanical cues. *J Pathol* 2014;**233:** 183-195.

37. Khan T, Muise ES, Iyengar P, Wang ZV, Chandalia M, Abate N*, et al.* Metabolic Dysregulation and Adipose Tissue Fibrosis: Role of Collagen VI. *Mol Cell Biol* 2009;**29:** 1575-1591.

38. Marcelin G, Ferreira A, Liu Y, Atlan M, Aron-Wisnewsky J, Pelloux V*, et al.* A PDGFRα-Mediated Switch toward CD9(high) Adipocyte Progenitors Controls Obesity-Induced Adipose Tissue Fibrosis. *Cell Metab* 2017;**25:** 673-685.

39. Spencer M, Yao-Borengasser A, Unal R, Rasouli N, Gurley CM, Zhu B*, et al.* Adipose tissue macrophages in insulin-resistant subjects are associated with collagen VI and fibrosis and demonstrate alternative activation. *Am J Physiol Endocrinol Metab* 2010;**299:** E1016-1027.

40. Scharenberg MA, Pippenger BE, Sack R, Zingg D, Ferralli J, Schenk S*, et al.* TGF-β-induced differentiation into myofibroblasts involves specific regulation of two MKL1 isoforms. *J Cell Sci* 2014;**127:** 1079-1091.

41. Sun K, Halberg N, Khan M, Magalang UJ, Scherer PE. Selective Inhibition of Hypoxia-Inducible Factor 1α Ameliorates Adipose Tissue Dysfunction. *Mol Cell Biol* 2013;**33:** 904.

42. Halberg N, Khan T, Trujillo ME, Wernstedt-Asterholm I, Attie AD, Sherwani S*, et al.* Hypoxia-inducible factor 1alpha induces fibrosis and insulin resistance in white adipose tissue. *Mol Cell Biol* 2009;**29:** 4467-4483.

43. Perry RJ, Camporez JG, Kursawe R, Titchenell PM, Zhang D, Perry CJ*, et al.* Hepatic acetyl CoA links adipose tissue inflammation to hepatic insulin resistance and type 2 diabetes. *Cell* 2015;**160:** 745-758.

44. Cifarelli V, Beeman SC, Smith GI, Yoshino J, Morozov D, Beals JW*, et al.* Decreased adipose tissue oxygenation associates with insulin resistance in individuals with obesity. *J Clin Invest* 2020;**130:** 6688-6699.

Table

Table 1: Participant characteristics from the entire cohort and sub-cohort analysis. Values expressed as mean±SD. Plasma concentrations were evaluated after an overnight fast. HS, High FA Ra suppression, LS, Low FA Ra suppression, HOMA-IR, homeostatic model assessment for insulin resistance, NEFA, non-esterified fatty acids, HDL, high-density lipoprotein. * p<0.05 versus HS sub-cohort.

	All participants	**Sub-cohort analysis**		
	n=66	**HS** (n=8)	**LS** (n=8)	*p*
Sex	F=46, M=20	F=6, M=2	F=6, M=2	-
Age (years)	31 ± 7	31 ± 6	32 ± 5	0.85
Body mass (kg)	96.9 ± 12.2	94.7 ± 9.6	94.9 ± 8.7	0.96
Fat mass (kg)	42.1 ± 6.7	40.7 ± 4.7	40.8 ± 5.8	0.99
Fat free mass (kg)	54.7 ± 9.5	53.9 ± 9.7	54.2 ± 9.1	0.96
Body fat %	43.5 ± 5.4	43.3 ± 5.7	43.1 ± 6.1	0.95
BMI (kg/m^2)	34.0 ± 3.0	34.0 ± 2.6	33.8 ± 2.6	0.87
Glucose (mmol/l)	4.9 ± 0.5	4.6 ± 0.4	4.8 ± 0.6	0.40
Insulin (µU/ml)	16.2 ± 9.7	7.0 ± 2.2	19.2 ± 10*	<0.01
HbA1c (%)	5.3 ± 0.4	5.1 ± 0.2	5.5 ± 0.6	0.13
HOMA-IR	3.6 ± 2.3	1.4 ± 0.5	4.2 ± 2.5*	0.010
NEFA (µmol/l)	432 ± 169	378 ± 99	403 ± 164	0.72

Triacylgycerol (mmol/l)	0.98 ± 0.6	0.6 ± 0.2	1.1 ± 0.4*	0.015
HDL (mmol/l)	1.02 ± 0.3	1.17 ± 0.4	0.95 ± 0.2	0.17

Figure Legends

Figure 1: Insulin-mediated glucose uptake and lipid kinetics across all participants (n=66). A) Insulin-mediated glucose uptake. B) Basal glycerol Ra. C) Clamp glycerol Ra. D) Insulin-mediated glycerol Ra suppression. E) Basal fatty acid Ra. F) Clamp FA Ra. G) Insulin-mediated FA Ra suppression.

Figure 2: Clinical and deep phenotyping factors associated with insulin-mediated glucose uptake. A) Lasso regression coefficients for clinical factors associated with insulin-mediated glucose uptake. B) Lasso regression coefficients for deep phenotyping factors (i.e., substrate control and oxidation under fasting and hyperinsulinemia), and insulin-mediated glucose uptake. C) Independent correlation (Pearson's) for all individual factors associated with insulin-mediated glucose uptake, adjusted for age and sex (partial r). D-F) Relationships between insulin-mediated glucose uptake and FA Ra suppression (D), insulin-mediated FA Ra (clamp) normalized to fat mass (E), and fat free mass (F). * Significant correlation versus insulin-mediated glucose uptake (nmol/kg FFM/min) / (μU/mL)) when adjusted for multiple comparisons (p.adjust < 0.05). n=66.

Figure 3: Relationships between adipose tissue cell size and insulin sensitivity. Association between mean adipocyte size and A) insulin-mediated glucose uptake, B) FA Ra suppression. C) Adipocyte cell size distribution from study cohort (bins=30). D) Representative image for a participant with high (513 nmol/kg FFM/min/ (μU/mL)) and

low (270 nmol/kg FFM/min/ (μU/mL)) insulin-mediated glucose uptake, scale bar = 100μm. Association between the frequency of small adipocytes (1000-3196μm^2) and E) insulin-mediated glucose uptake, F) FA Ra suppression. Association between the frequency of large adipocytes (> 6784μm^2) and G) insulin-mediated glucose uptake, H) FA Ra suppression. n=58.

Figure 4: Comparison of insulin-mediated glucose uptake, hepatic insulin sensitivity, liver fat, and visceral fat area from a sub-cohort matched for body composition, and discordant FA Ra suppression. A) Participants of discordant FA Ra suppression and well-matched for body composition and sex were paired into 'High FA Ra Suppression' (HS) and 'Low FA Ra suppression' (LS) sub-cohorts. B) FA Ra measured under basal and during the hyperinsulinemic-euglycemic clamp. C-D) Measures of insulin-mediated glucose uptake normalized to insulin (nmol/kg FFM/min/insulin: C), and not normalized to insulin (μmol/kg FFM/min: D). E) Glucose Ra measured before and during hyperinsulinemic-euglycemic clamp. F) Hepatic insulin sensitivity measured as glucose Ra suppression during the hyperinsulinemic-euglycemic clamp. G-H) Liver fat % (G), and visceral fat area (cm^2) between groups (H). I) Association between liver fat % and FA Ra suppression for all study participants. J) Association between visceral fat area and FA Ra suppression for all study participants. Data are mean±SD. * $p<0.05$ HS versus LS. † $p< 0.05$ basal versus clamp (insulin-stimulated) during hyperinsulinemic-euglycemic clamp. n=16.

Figure 5: Comparison of adipose tissue proteome in HS versus LS sub-cohorts. A) Overview of proteomic workflow. B) Volcano plot showing differentially expressed proteins between groups ($p<0.05$, abundance ratio>1.5), and arrows indicating the number of proteins differentially expressed between groups. C) MA plots demonstrating differentially expressed proteins with respect to integrative abundance. D) Kyoto encyclopedia of genes and genomes (KEGG) pathway enrichment (top ten). E) Differentially expressed proteins from ECM-receptor interaction KEGG pathway. F) Protein expression for COL6A protein (∑COL6A1, COL6A2, COL6A3), and G) TGFβ1. Data are mean±SD. * $p<0.05$ and abundance ratio ≥1.5. n=16.

Figure 6: Relationships between insulin sensitivity and skeletal muscle lipidomic profile. A) Hierarchical clustering heatmap of lipids association with insulin-mediated glucose uptake and FA Ra suppression, (k=5). B) Venn-diagram of significant lipids grouped in cluster 1 - negative association with both insulin-mediated glucose uptake and FA Ra suppression, and cluster 5 - positive association with both insulin-mediated glucose uptake and FA Ra suppression. C) Significant association between individual lipid species for both insulin-mediated glucose uptake and FA Ra suppression. Significant values adjusted for multiple comparisons. n =18.

Figure 7: Relationships between skeletal muscle free fatty acid, acylcarnitine, diacylglycerol, and triacylglycerol chain-length versus insulin-mediated glucose uptake$_z$, and FA Ra suppression$_z$. (A-B) Relationships between beta coefficients describing models between acyl-chain lengths of skeletal muscle free fatty acids, (C-D) acylcarnitine, (E-F) DAG, and (G-H) TAG on insulin-mediated glucose uptake$_z$ and FA Ra Suppression$_z$. Individual data points represent each species within respective class of lipids. n =18.

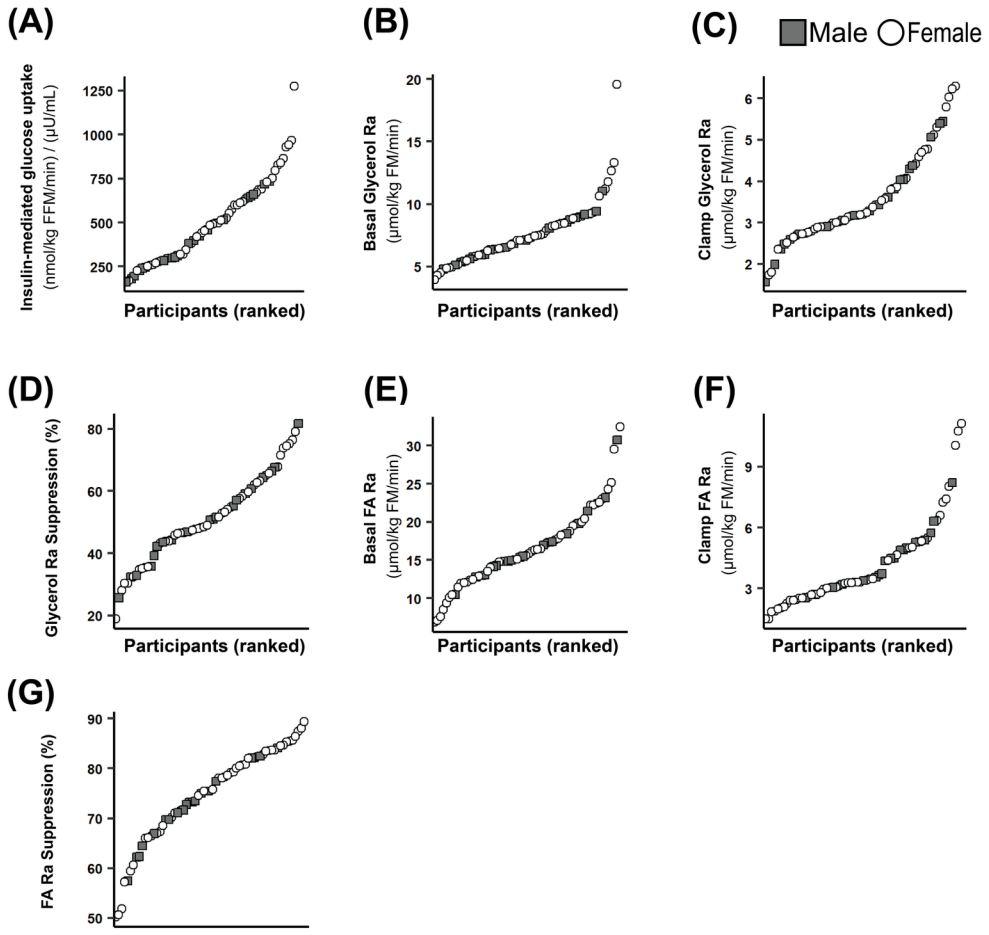

OBY_23734_Schleh-AdiposeTissueAndInsulinSensitivity-Figure1.png

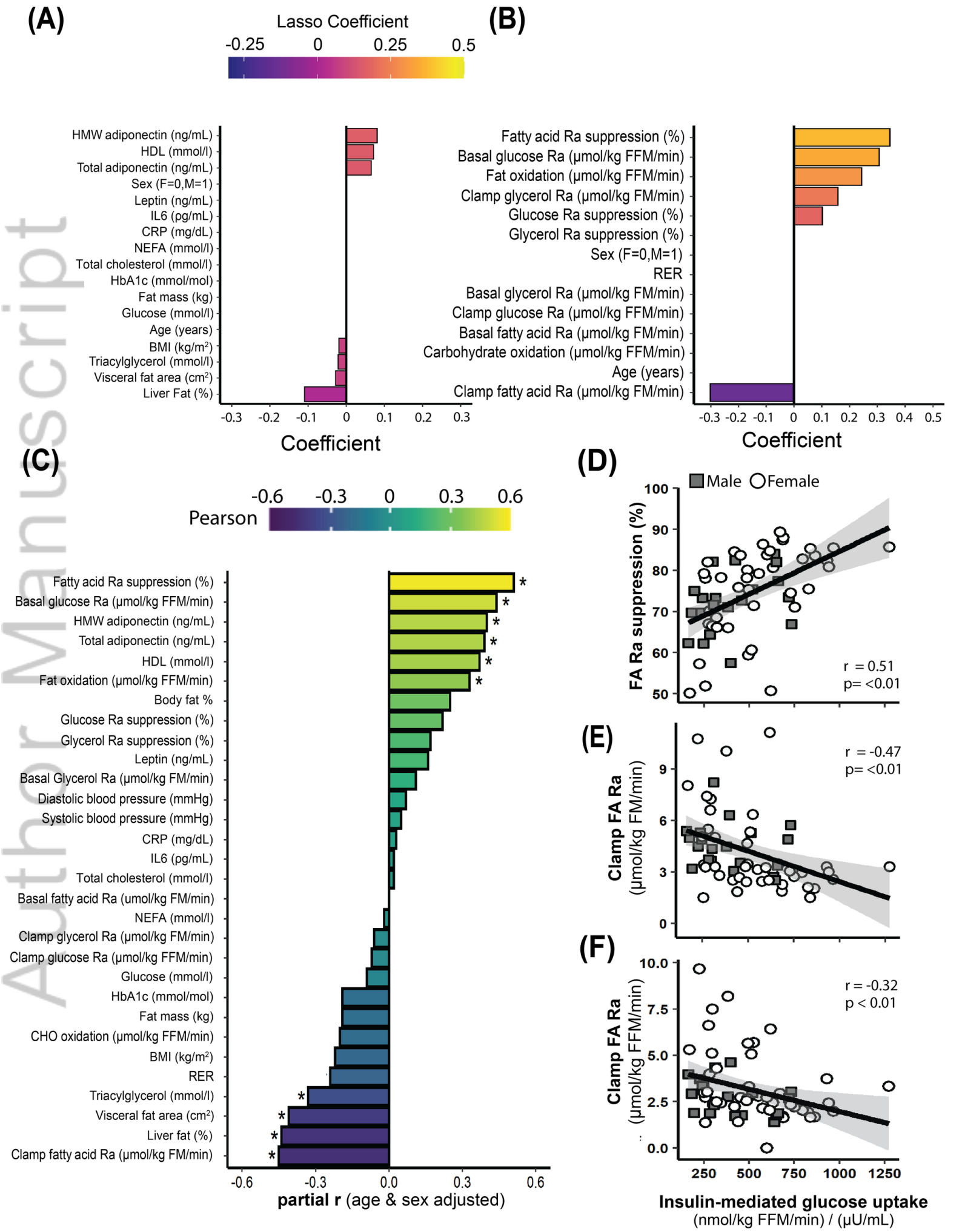

OBY_23734_Schleh-AdiposeTissueAndInsulinSensitivity-Figure2.png

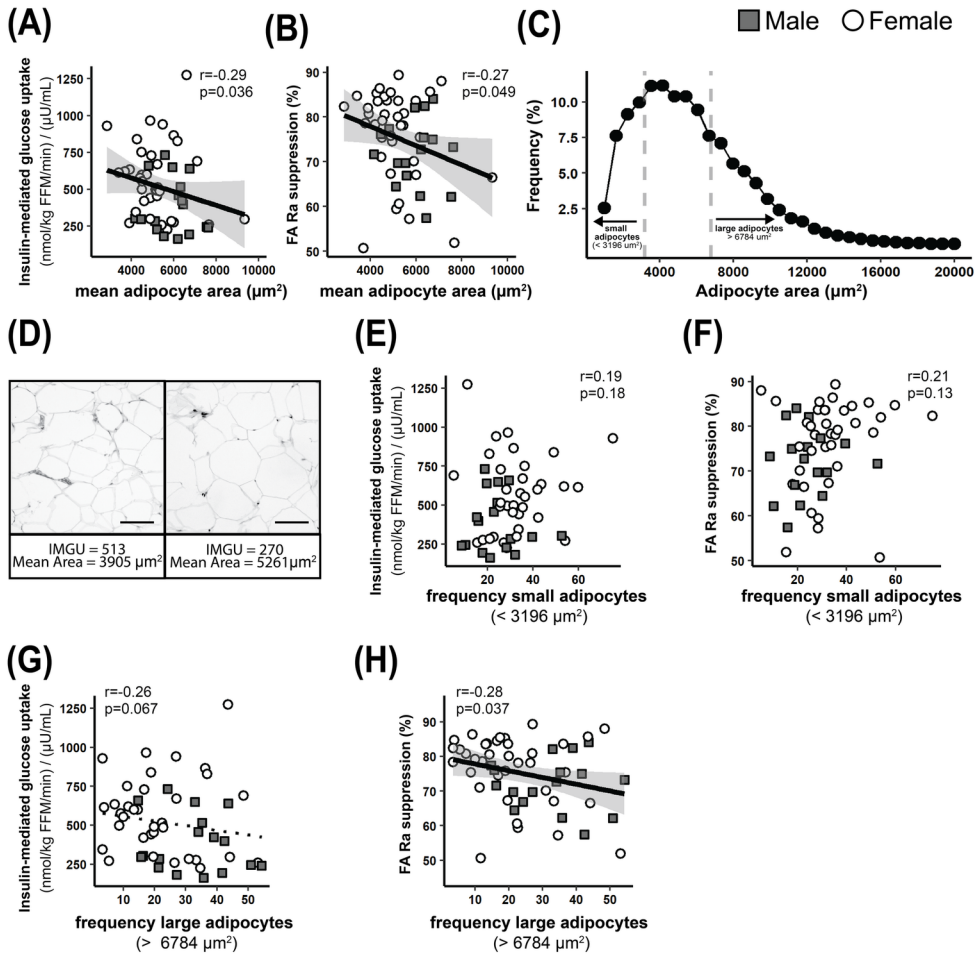

OBY_23734_Schleh-AdiposeTissueAndInsulinSensitivity-Figure3.png

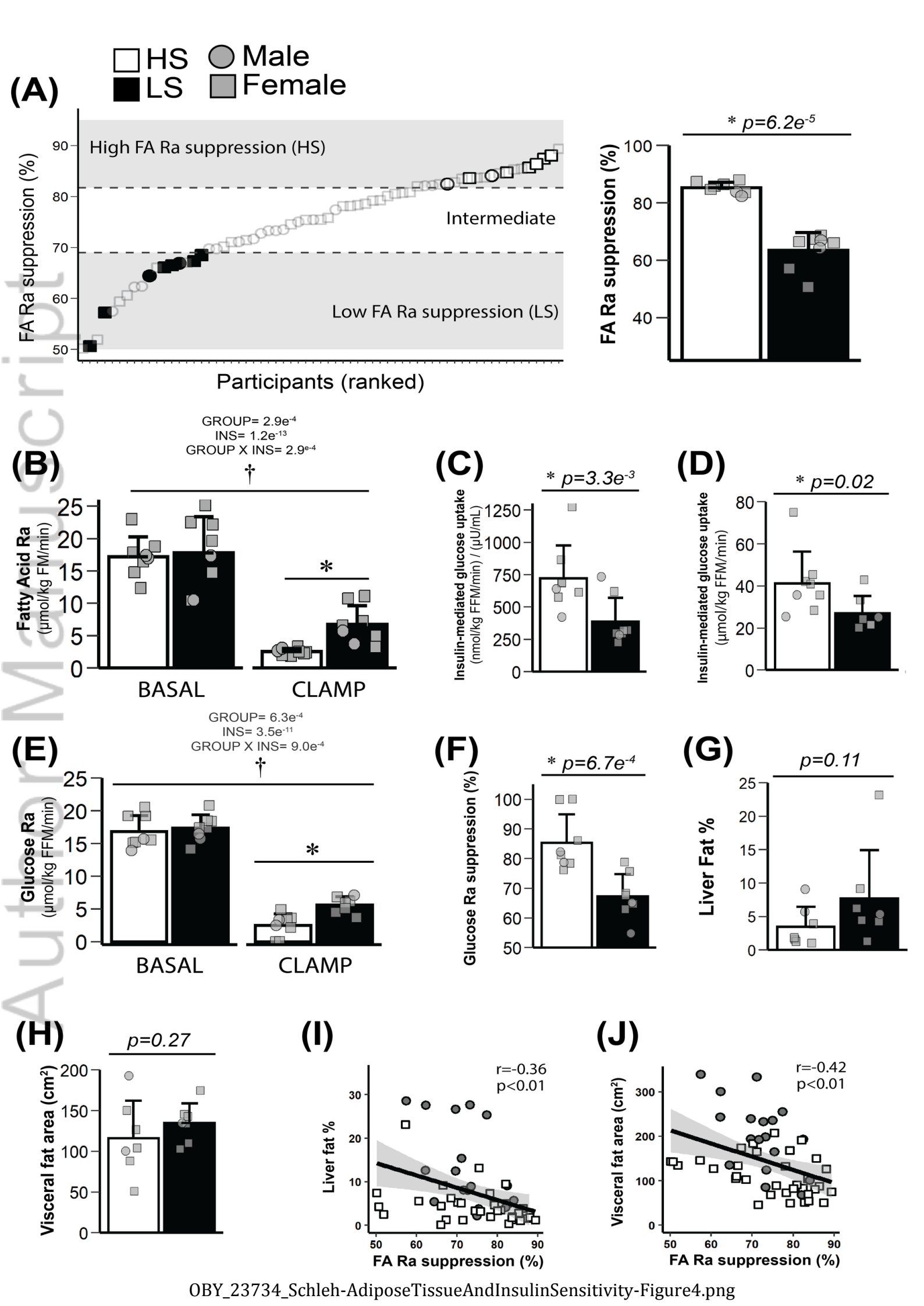

OBY_23734_Schleh-AdiposeTissueAndInsulinSensitivity-Figure4.png

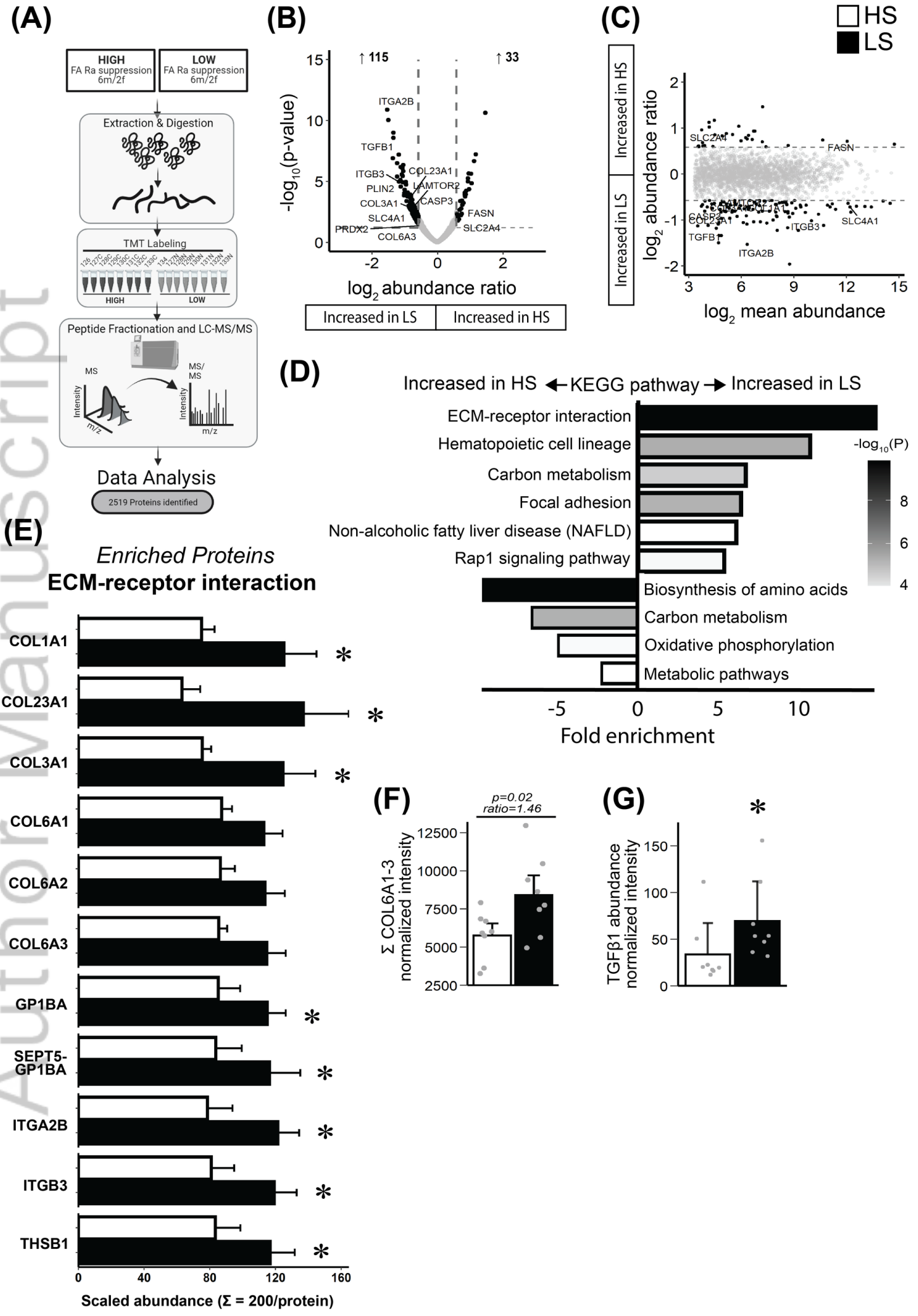

OBY_23734_Schleh-AdiposeTissueAndInsulinSensitivity-Figure5.png

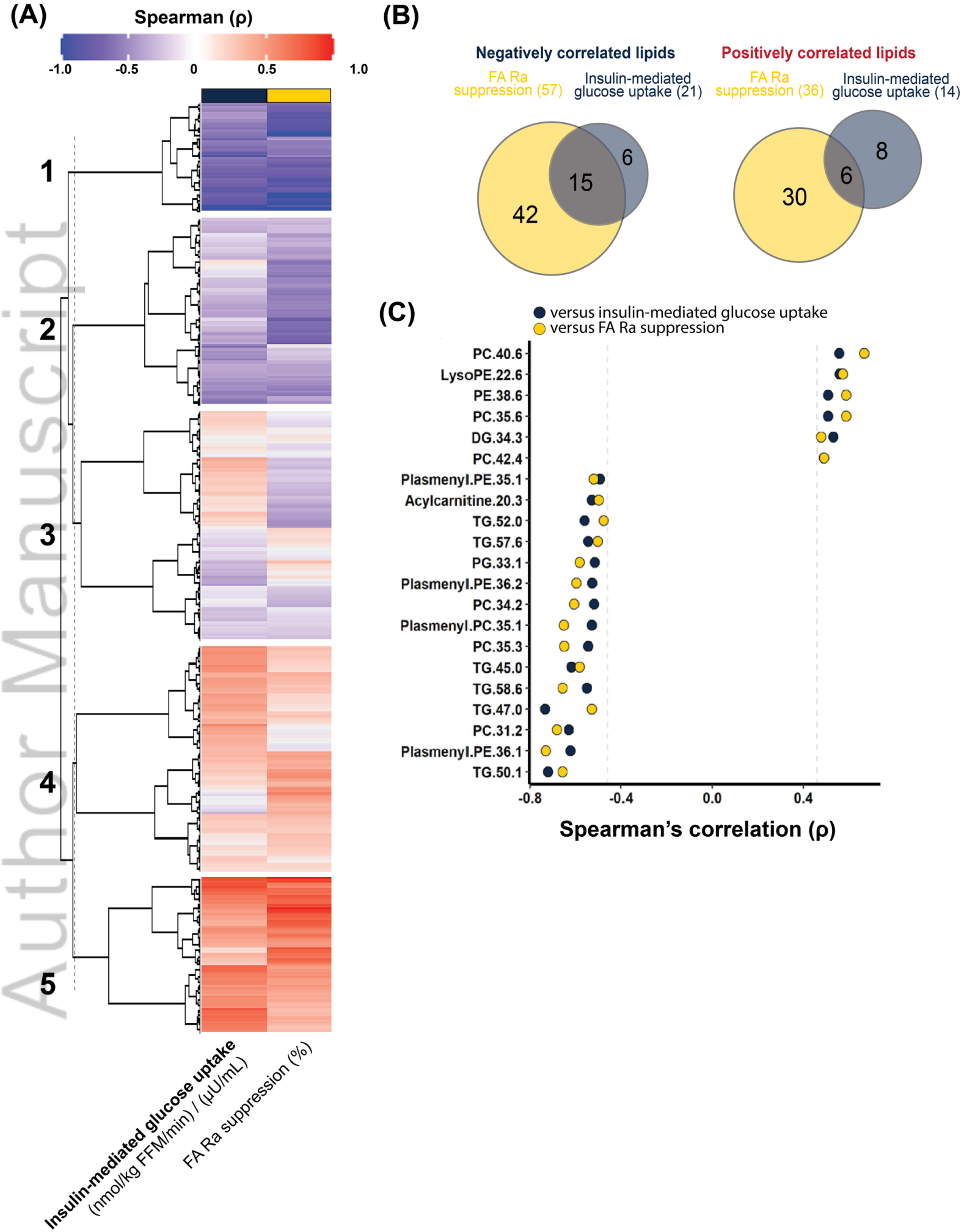

OBY_23734_Schleh-AdiposeTissueAndInsulinSensitivity-Figure6.png

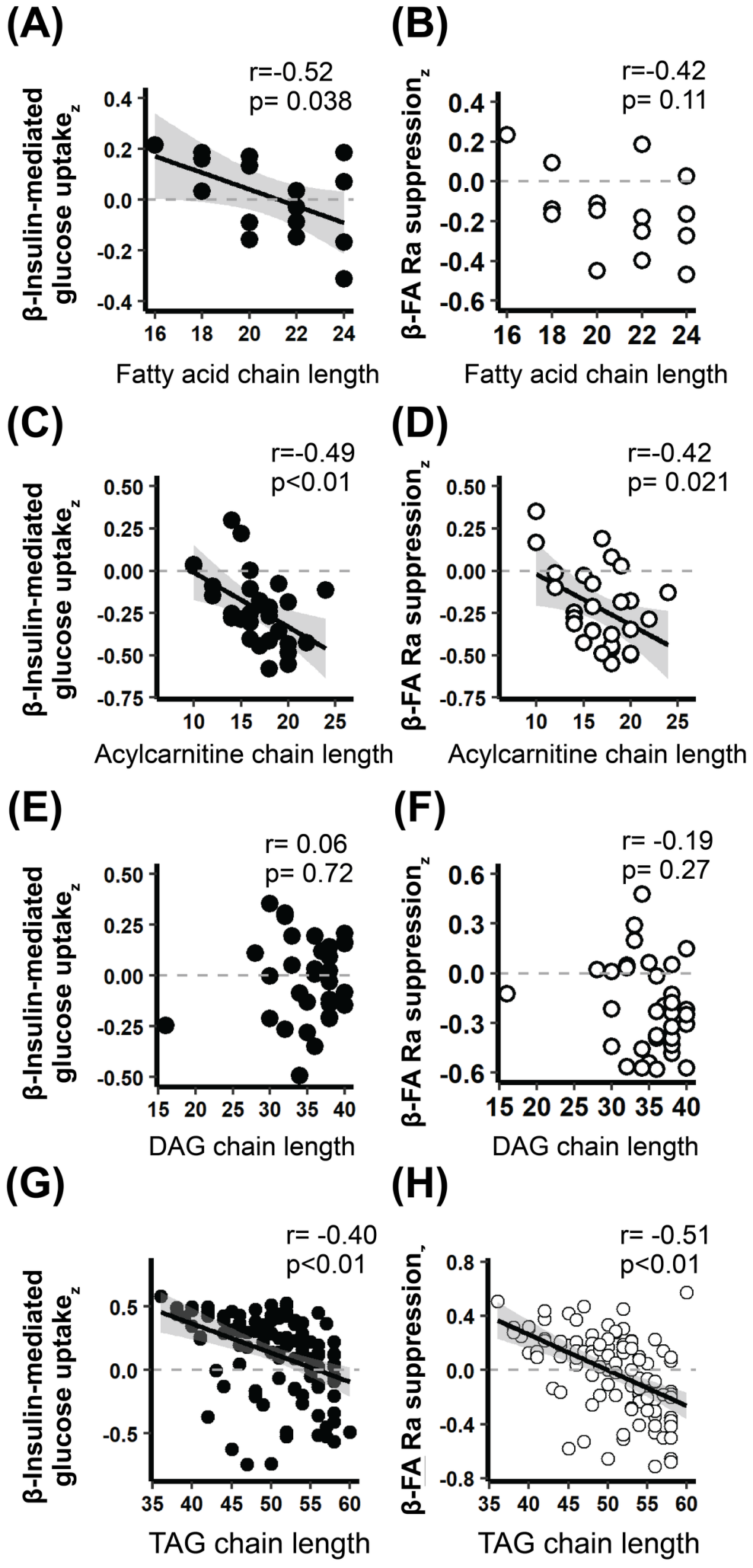

OBY_23734_Schleh-AdiposeTissueAndInsulinSensitivity-Figure7.png